Supporting information for the article:

Vujančević, J., Andričević, P., Bjelajac, A., Đokić, V., Popović, M., Rakočević, Z., Horváth, E., Kollár, M., Náfrádi, B., Schiller, A., Domanski, K., Forró, L., Pavlović, V., Janaćković, Đ., 2019. Dry-pressed anodized titania nanotube/CH3NH3PbI3 single crystal heterojunctions: The beneficial role of N doping. Ceramics International 45, 10013–10020. https://doi.org/10.1016/j.ceramint.2019.02.045

Supporting information

Dry-pressed anodized titania nanotube/$CH_3NH_3PbI_3$ single crystal heterojunctions: the beneficial role of N doping

*Jelena Vujančević [a], Pavao Andričević [b], Anđelika Bjelajac [c], Veljko Đokić [d], Maja Popović [e], Zlatko Rakočević [e], Endre Horváth *[b], Márton Kollár [b], Bálint Náfrádi [b], Andreas Schiller [f], Kondrad Domanski [f], László Forró [b], Vera Pavlović [g], Đorđe Janaćković [d]*

[a] Institute of Technical Sciences of SASA, Knez Mihailova 35/IV, 11000 Belgrade, Serbia

[b] Ecole Polytechnique Fédérale de Lausanne, Laboratory of Physics of Complex Matter (LPMC), CH-1015 Lausanne, Switzerland

[c] University of Belgrade, Innovation Center of Faculty of the Technology and Metallurgy, Karnegijeva 4, 11000 Belgrade, Serbia

[d] University of Belgrade, Faculty of Technology and Metallurgy, Karnegijeva 4, 11000 Belgrade, Serbia

[e] University of Belgrade, Vinča Institute of Nuclear Sciences, Laboratory of Atomic Physics, Mike Alasa 12-14, 11001 Belgrade, Serbia

[f] Fluxim AG, Katharina-Sulzer-Platz 2, 8400 Winterthur

[g] University of Belgrade, Faculty of Mechanical Engineering, Kraljice Marije 16, 11000 Belgrade, Serbia

[*]Corresponding author. Tel. +41 21 6934515, Fax. +41 21 6934470, endre.horvath@epfl.ch

Table S1. Reported methods for nitrogen doping of anodized TiO_2 nanotube arrays.

Methods	*Nitrogen content, at.%*	*Improvement*	*Reference*
Hydrothermal process **Source: triethylamine**	0.25	Photoelectrochemical activity and photocatalytic degradation of RhB	Sun et al.[1]
Hydrothermal process **Source: diethylenetriamine**	0.5 - 2.2	Photoelectrochemical water splitting	Hejazi et al. [2]
Immersing in 1M NH_3 for 10 h, followed by annealing in air	-	Photocatalytic degradation of MO	Yuan et al. [3]
N^+-ion implantation into Ti foil and then Ti foil was anodized in order to obtain N-TiO_2 nanotubes	-	Improved photocurrent	Hou et al. [4]
N^+-ion implantation of TiO_2 nanotube arrays	-	Improved photocurrent	Ghicov et al. [5]
Anodization in the organic electrolyte with urea as a nitrogen source	0.22 - 0.50	Photocatalytic degradation of phenol	Mazierski et al. [6]
Annealing in N_2 atmosphere at 450 °C, 3 h, different gas flow	0 - 9.47	Photocatalytic degradation of MB	Le et al. [7]
Annealing in NH_3 atmosphere at 300-600 °C	-	Increased photocurrent	Vitiello et al. [8]
Annealing in NH_3 atmosphere at 550 °C, 5h	9	Improved field emission current density	Liu et al. [9]
First annealing in air at 450 °C and then in NH_3 at 500 °C	1.9	Photocatalytic degradation of MB	Wang et al. [10]
Annealing in NH_3 atmosphere at 450 °C, 30 min	1	-	Bjelajac et al. [11]

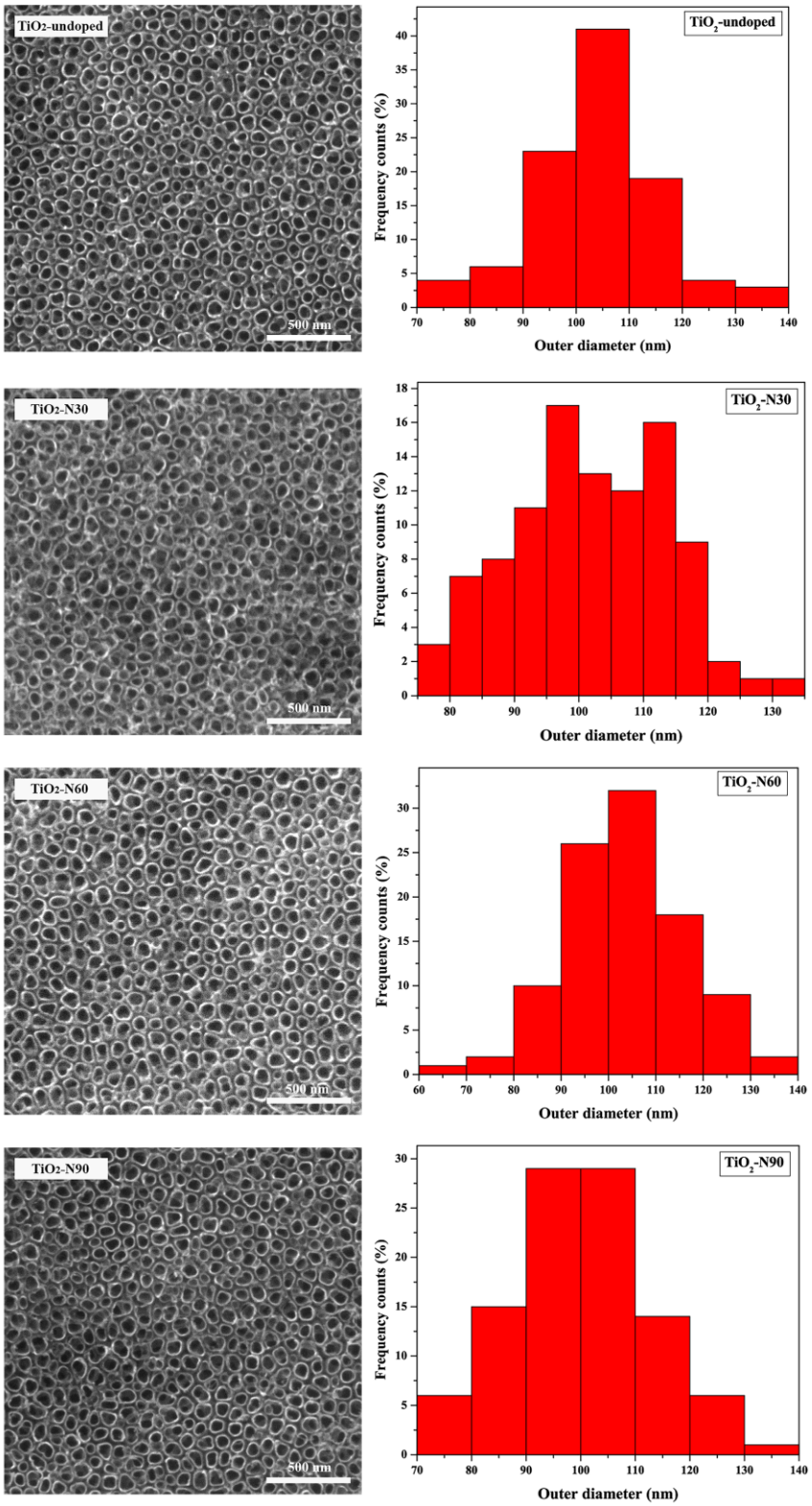

Figure S1. SEM images and statistical distributions of outer diameters obtained by analyzing SEM micrographs of 100 nanotubes.

Table S2. Average morphology parameters for TiO_2-undoped, TiO_2-N30, TiO_2-N60 and TiO_2-N90 samples.

Samples	***Outer diameter with standard deviation, nm***	***Inner diameter with standard deviation, nm***	***Wall thickness with standard deviation, nm***
TiO_2-undoped	103 (11)	75 (10)	13 (2)
TiO_2-N30	101 (11)	73 (11)	13 (2)
TiO_2-N60	103 (12)	76 (10)	13 (2)
TiO_2-N90	100 (12)	75 (16)	12 (2)

Table S3. Average crystals size for TiO_2-undoped, TiO_2-N30, TiO_2-N60 and TiO_2-N90 samples.

Samples	**Crystal size for anatase (101), nm**
TiO_2-undoped	18
TiO_2-N30	19
TiO_2-N60	20
TiO_2-N90	23

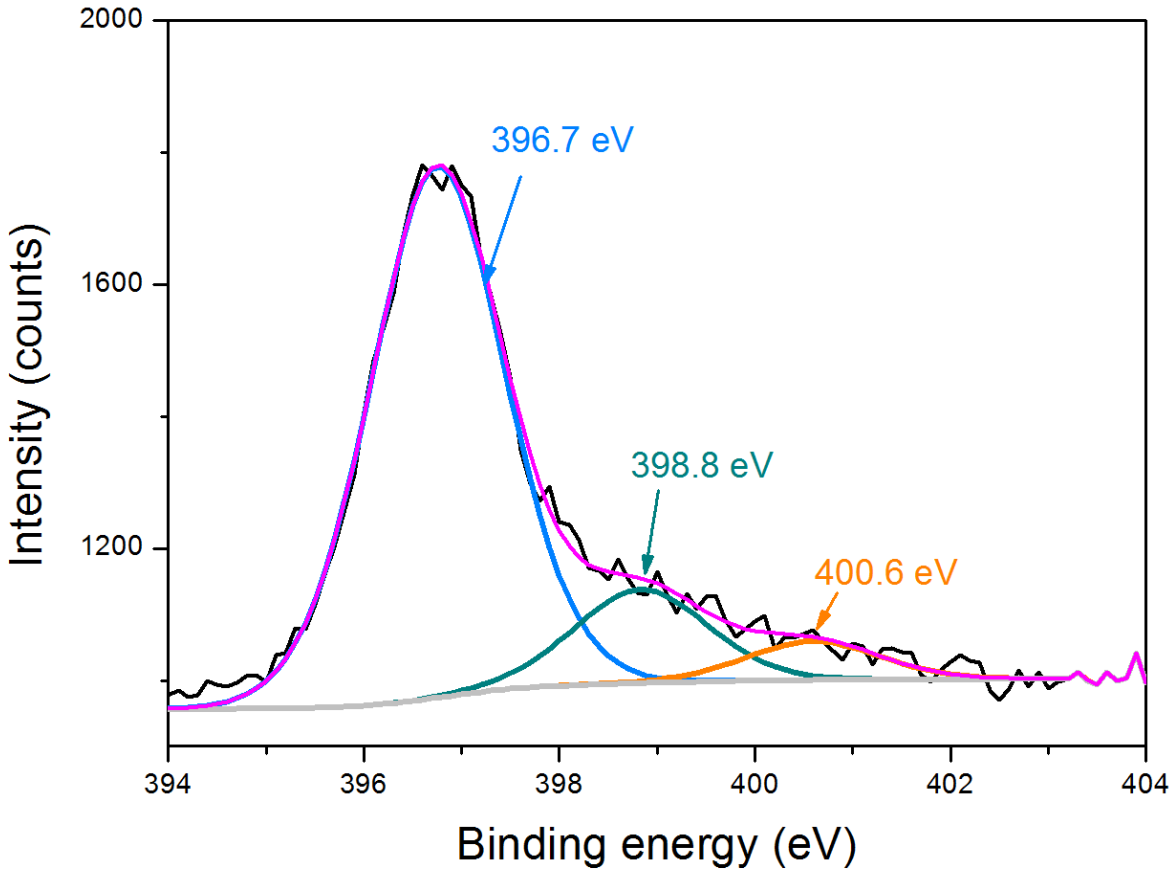

Figure S2. Deconvoluted XPS spectra of N 1s core level of Ti foil (black line-experimental, grey line-background, magenta line-envelope).

Table S4. Peak positions and atomic percentages of N1s core levels for TiO_2-undoped, TiO_2-N30, TiO_2-N60 and TiO_2-N90 samples.

Samples	***Substitutional nitrogen***		***Interstitial nitrogen***		***Chemisorbed nitrogen***	
	B.E. (eV)	at.%	B.E. (eV)	at.%	B.E. (eV)	at.%
TiO_2-undoped	/	/	399.8	0.75	401.9	0.15
TiO_2-N30	396.0	0.18	399.8	1.42	401.9	0.43
TiO_2-N60	396.3	0.45	399.7	1.10	401.5	0.39
TiO_2-N90	396.2	0.35	399.8	0.79	/	/

Table S5. Positions and atomic percentages of Ti $2p_{3/2}$ and O1s core peaks for TiO_2-undoped, TiO_2-N30, TiO_2-N60 and TiO_2-N90 samples.

Samples	***Ti $2p_{3/2}$***	***O 1s***					
	B.E.(eV)	Peak 1 B.E. (eV)	at.%	Peak 2 B.E. (eV)	at.%	Peak 3 B.E. (eV)	at.%
TiO_2-undoped	458.8	530.0	83.42	531.3	10.78	532.3	5.79
TiO_2-N30	458.9	530.1	75.86	531.6	15.61	532.5	8.53
TiO_2-N60	458.8	530.1	83.50	531.5	11.99	532.5	4.51
TiO_2-N90	458.7	530.0	85.49	531.4	10.86	532.3	3.64

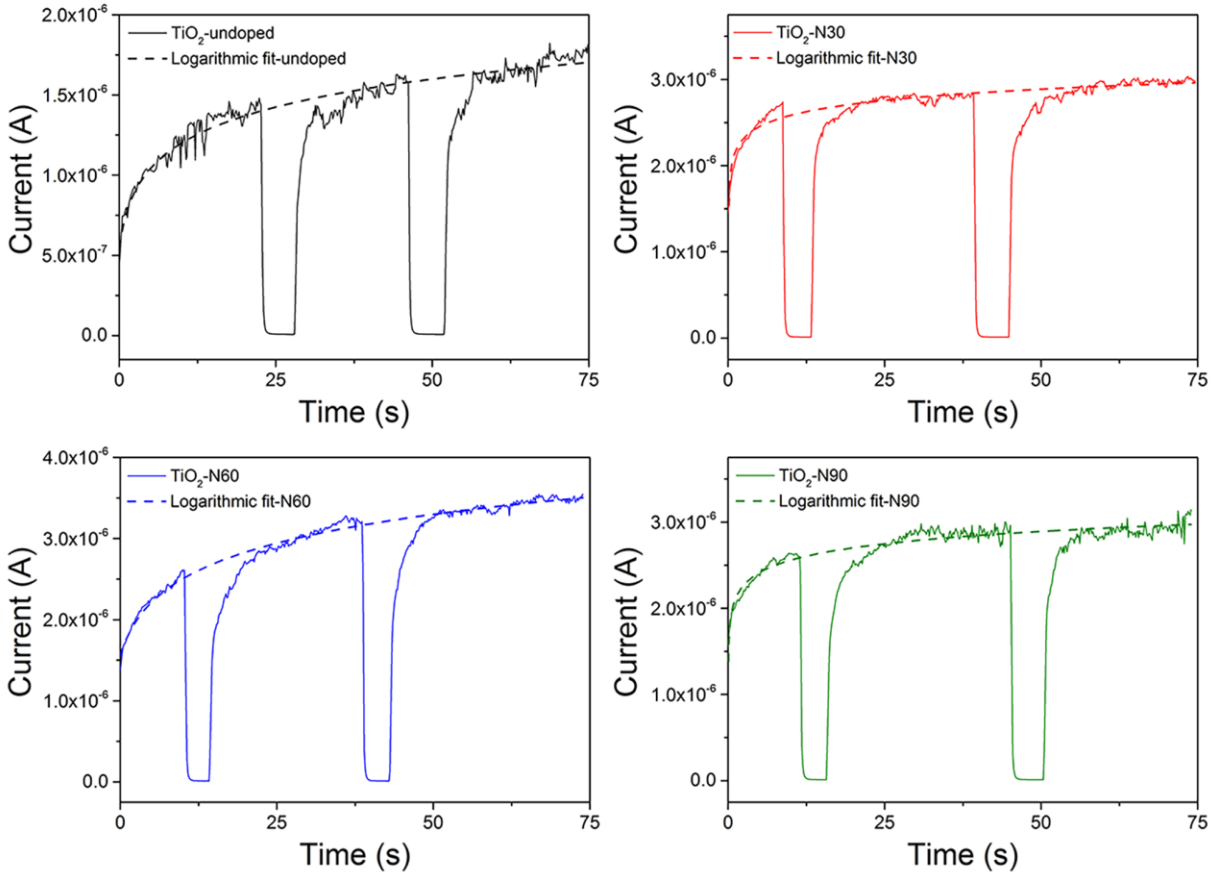

Figure S3. The time evolution of the current during the preconditioning of the TiO_2/perovskite sample at a bias voltage of 100 V for 75 sec. Dashed line is the logarithmic fit of the base line of the current time evolution.

Before each I-V measurement the sample was preconditioned applying a 100 V bias voltage for 75 seconds. As a result the conductivity of the perovskite crystal increases and stabilizes giving us a constant and comparable signal for all samples. As it is known, perovskite crystals experience ion migration when exposed to a large electric field [12]. While performing I-V measurements, scanning the voltage to 10 V, ion migration takes place resulting in large hysteresis and increasing values of current for each repeated measurement, using the same crystal. By applying a voltage high enough for a sufficient time interval we assure that the

perovskite crystal is in the same state before every measurement. The same technique was previously used by Yi et al. [13] to perform Hall Effect measurements on perovskite single crystals. The preconditioning is performed in ambient conditions under a white fluorescence light source of 1.83 mW/mm^2, with short dark intervals to check the photoresponse characteristics of the perovskite crystal. A logarithm function is fitted to follow the current rise under light (Figure S3).

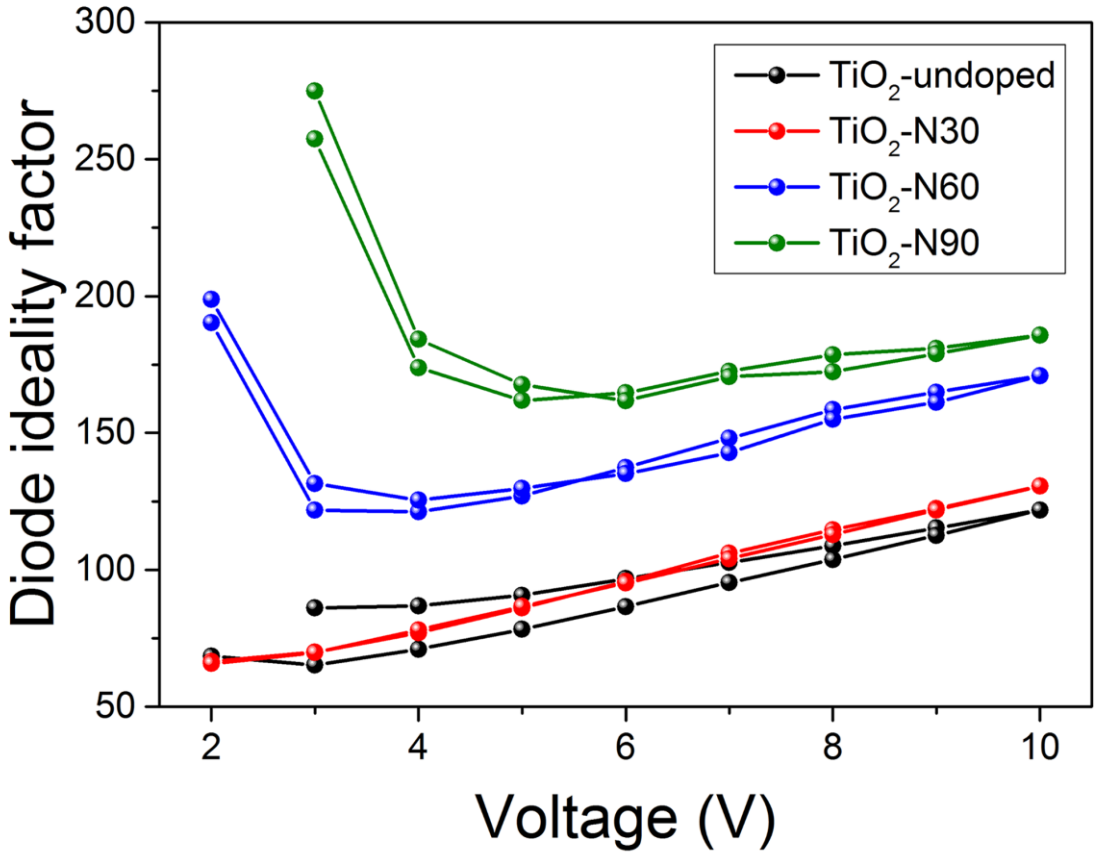

Figure S4. Ideality factor for TiO_2-undoped, TiO_2-N30, TiO_2-N60 and TiO_2-N90 samples.

The ideality factor of a diode is a measure of how closely the diode follows the ideal diode equation. The derivation of the simple diode equation uses certain assumption about the cell. In

practice, there are second order effects so that the diode does not follow the simple diode equation and the ideality factor provides a way of describing them. The following equation is called the Shockley ideal diode equation:

$$I = I_S\left(e^{\frac{V_D}{nV_T}} - 1\right)$$

where I is the diode current, I_S is the reverse bias saturation current, V_D is the voltage across the diode, V_T is the thermal voltage and n the ideality factor, also known as the quality factor. The ideality factor n typically varies from 1 to 2 (though can be higher in some cases), depending on the fabrication process and semiconductor material and is set to be equal to 1 for the case of an "ideal" diode. The ideality factor was added to account for imperfect junctions as observed in real transistors. The factor mainly accounts for carrier recombination, as the charge carriers cross the depletion region. The thermal voltage V_T is approximately 25.85 mV at 300 K, while a temperature close to "room temperature" is commonly used in device simulation software. For even rather small *forward bias* voltages the exponential is very large, since the thermal voltage is very small in comparison. The subtracted '1' in the diode equation is then negligible and the forward diode current can be approximated by

$$I = I_S e^{\frac{V_D}{nV_T}} \qquad (1)$$

From our I-V measurements the ideality factor was calculated using equation (1) and the results are shown in Figure S4.

References

[1] L. Sun, J. Cai, Q. Wu, P. Huang, Y. Su, C. Lin, N-doped TiO_2 nanotube array photoelectrode for visible-light-induced photoelectrochemical and photoelectrocatalytic activities, Electrochim. Acta. 108 (2013) 525–531. doi:10.1016/j.electacta.2013.06.149.

[2] S. Hejazi, N. Truong Nguyen, A. Mazare, P. Schmuki, Aminated TiO_2 nanotubes as a photoelectrochemical water splitting photoanode, Catal. Today. 281 (2017) 189–197. doi:10.1016/j.cattod.2016.07.009.

[3] B. Yuan, Y. Wang, H. Bian, T. Shen, Y. Wu, Z. Chen, Nitrogen doped TiO_2 nanotube arrays with high photoelectrochemical activity for photocatalytic applications, Appl. Surf. Sci. 280 (2013) 523–529. doi:10.1016/j.apsusc.2013.05.021.

[4] X. Hou, F. Liu, K. Yao, H. Ma, J. Deng, D. Li, B. Liao, Photoelectrical properties of nitrogen doped TiO_2 nanotubes by anodic oxidation of N^+ implanted Ti foils, Mater. Lett. 124 (2014) 101–104. doi:10.1016/j.matlet.2014.03.050.

[5] A. Ghicov, J.M. Macak, H. Tsuchiya, J. Kunze, V. Haeublein, L. Frey, P. Schmuki, Ion implantation and annealing for an efficient N-doping of TiO_2 nanotubes, Nano Lett. 6 (2006) 1080–1082. doi:10.1021/nl0600979.

[6] P. Mazierski, M. Nischk, M. Gołkowska, W. Lisowski, M. Gazda, M.J. Winiarski, T. Klimczuk, A. Zaleska-Medynska, Photocatalytic activity of nitrogen doped TiO_2 nanotubes prepared by anodic oxidation: The effect of applied voltage, anodization time and amount of nitrogen dopant, Appl. Catal. B Environ. 196 (2016) 77–88. doi:10.1016/j.apcatb.2016.05.006.

[7] P.H. Le, L.T. Hieu, T.-N. Lam, N.T.N. Hang, N.V. Truong, L.T.C. Tuyen, P.T. Phong, J. Leu, Enhanced photocatalytic performance of nitrogen-doped TiO_2 nanotube arrays using a simple annealing process, Micromachines. 9 (2018) 618. doi:10.3390/mi9120618.

[8] R.P. Vitiello, J.M. Macak, A. Ghicov, H. Tsuchiya, L.F.P. Dick, P. Schmuki, N-doping of anodic TiO_2 nanotubes using heat treatment in ammonia, Electrochem. Commun. 8 (2006) 544–548. doi:10.1016/j.elecom.2006.01.023.

[9] G. Liu, F. Li, D.-W. Wang, D.-M. Tang, C. Liu, X. Ma, G.Q. Lu, H.-M. Cheng, Electron field emission of a nitrogen-doped TiO_2 nanotube array, Nanotechnology. 19 (2008) 025606. doi:10.1088/0957-4484/19/02/025606.

[10] H. Wang, Y. Yang, J. Wei, L. Le, Y. Liu, C. Pan, P. Fang, R. Xiong, J. Shi, Effective photocatalytic properties of N doped titanium dioxide nanotube arrays prepared by anodization, React. Kinet. Mech. Catal. 106 (2012) 341–353. doi:10.1007/s11144-012-0439-z.

[11] A. Bjelajac, V. Djokić, R. Petrović, N. Bundaleski, G. Socol, I.N. Mihailescu, Z. Rakočević, D. Janaćković, Absorption boost of TiO_2 nanotubes by doping with N and sensitization with CdS quantum dots, Ceram. Int. 43 (2017) 15040–15046. doi:10.1016/j.ceramint.2017.08.029.

[12] P. Calado, A.M. Telford, D. Bryant, X. Li, J. Nelson, B.C. O'Regan, P.R.F. Barnes, Evidence for ion migration in hybrid perovskite solar cells with minimal hysteresis, Nat. Commun. 7 (2016) 13831. doi:10.1038/ncomms13831.

[13] H.T. Yi, X. Wu, X. Zhu, V. Podzorov, Intrinsic charge transport across phase transitions

in hybrid organo-inorganic perovskites, Adv. Mater. 28 (2016) 6509–6514. doi:10.1002/adma.201600011.